

# Thermo-mechanical behavior of prestressed concrete box girder at hydration age

Gang Zhang<sup>1a</sup>, Meichun Zhu<sup>\*2</sup>, Shuanhai He<sup>1a</sup> and Wei Hou<sup>1b</sup>

<sup>1</sup>School of Highway, Chang'an University, Xi'an 710064, Shaanxi, China

<sup>2</sup>Department of Civil Engineering, Shanghai Normal University, Shanghai 201418, China

(Received July 25, 2017, Revised August 10, 2017, Accepted August 19, 2017)

**Abstract.** Excessively elevated temperature can lead to cracks in prestressed concrete (PC) continuous bridge with box girder on the pier top at cement hydration age. This paper presents a case study for evaluating the behavior of PC box girder during the early hydration age using a two-stage computational model, in the form of computer program ANSYS, namely, 3-D temperature evaluation and determination of mechanical response in PC box girders. A numerical model considering time-dependent wind speed and ambient temperature in ANSYS for tracing the thermal and mechanical response of box girder is developed. The predicted results were compared to show good agreement with the measured data from the PC box girder of the Zhaoshi Bridge in China. Then, based on the validated numerical model three parameters were incorporated to analyze the evolution of the temperature and stress within box girder caused by cement hydration heat. The results of case study indicate that the wind speed can change the degradation history of temperature and stress and reduce peak value of them. The initial casting temperature of concrete is the most significant parameter which controls cracking of PC box girder on pier top at cement hydration age. Increasing the curing temperature is detrimental to prevent cracking.

**Keywords:** prestressed concrete box girder; hydration heat; FEM; test; thermo-mechanical behavior; parametric analysis

## 1. Introduction

Cracking in newly built reinforced concrete bridge structures has become a common phenomenon (Germaniuk *et al.* 2016, Yi *et al.* 2013a, b, 2012). However, cracking in prestressed concrete box girder is also being detected in China for several years now (see Fig. 1) (Zhang 2009). Different from reinforced concrete structures which consider cracks as a standard concrete performance, cracks are not permitted in prestressed concrete box girders. So, it is crucial to investigate the development of temperature gradients and stresses in the PC box girder during the course of concrete construction, and propose measures to prevent the occurrence of cracks.

Investigation on the cracks in Fig. 1 found that the highly probable cause was the internal thermal pressure produced by cement hydration heat (Heat is liberated when cement is mixed with water, and this heat is called the hydration heat). In past decades, numerous studies of cement hydration heat effects on concrete dams, foundations and other massive concrete structures have been conducted (EI-Tayeb *et al.* 2017, Schackow *et al.* 2016, Wang *et al.* 2015, Gilbert 2017, Kodur *et al.* 2016, Zhu 2013, Kuriakose *et al.* 2016, Yun and Kim 2009, Fairbairn *et al.* 2004, Schutter *et al.* 2004, Estrada *et al.*

2006), but little research on PC box girder is reported (Krkoška and Moravčík 2015). In order to prevent cracks in massive concrete structures caused by the temperature of cement hydration heat, many techniques were developed to decrease cement hydration heat, such as adding pipe-cooling system and changing the cement content (Jin *et al.* 2001, Pepe *et al.* 2014, Chummuneerat *et al.* 2014). However, due to the structural complexity of PC box girder on the pier top, and large amount of steel and prestressing strands within girder body, and influence of high pier, water pipes used in pipe-cooling techniques are difficult to arrange within girder body to prevent cement hydration heat. Pre-cooling technique is commonly applied in construction of PC box girder on the pier top to reduce the initial casting temperature of concrete, by which some ice is added into the crude aggregate or cold water is used in mixture of concrete before casting. In addition, springing water is sometimes utilized in the process of concrete curing, to reduce the effect of hydration heat, including springing hot water (usually 45°C) or springing water at ambient temperature. The effect of the initial casting temperature and the curing temperature of concrete on cracking at early hydration age needs to be discussed.

The objective of this paper is to develop a three-dimensional finite element program for thermo-mechanical analysis of hydration heat in PC box girder. Finite element program ANSYS is applied to analyze the evolution of temperatures and stresses in a PC box girder on the pier top. The reliability of developed program is verified by comparing the calculated prediction results with the measured data from the actual PC box girder in the Zhaoshi Bridge in China. The validated model is applied to study the

\*Corresponding author, Associate Professor

E-mail: meichunzhu@163.com

<sup>a</sup>Professor

<sup>b</sup>Ph.D.

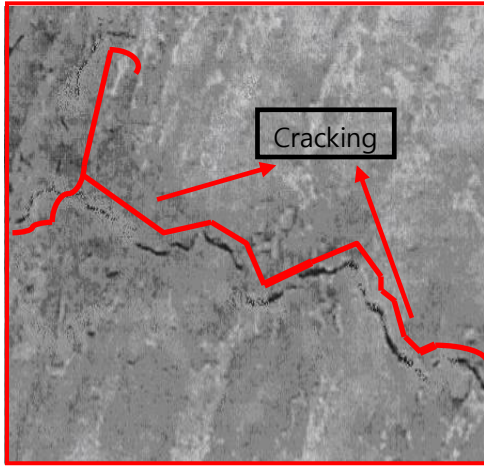


Fig. 1 Crack of PC box girder at early hydration age

effect of the wind speed, the initial casting temperature and the curing temperature on temperature rise and stress development in PC box girder during cement hydration age. Based on the parametric study, solutions are proposed to minimize the adverse effects of differential temperature rise due to cement hydration.

### 2. Finite element formulation

Computation of temperature rise caused by cement hydration during early stages of concrete curing and development of associated internal stress involves two main steps: thermal analysis and stress analysis. These two steps are to be conducted through a sequential thermo-mechanical analysis which is governed by different sets of differential equations.

The thermal analysis provides a spatial temperature distribution and temperature-time history for the desired duration of curing. The temperature computation as a function of time is listed as follows (Zhu 2013, Wang *et al.* 2002)

$$I = \iiint_R \frac{1}{2} \left( \left( \frac{\partial T}{\partial x} \right)^2 + \left( \frac{\partial T}{\partial y} \right)^2 + \left( \frac{\partial T}{\partial z} \right)^2 \right) + \frac{1}{\lambda} \left( \frac{\partial T}{\partial t} - \frac{\partial \theta}{\partial t} \right) T dV + \iint_{\Gamma} \frac{\beta}{k} T \left( \frac{T}{2} - T_a \right) d\Gamma \quad (1)$$

$$\lambda = \frac{k}{cp} \quad (2)$$

Where,  $I$  is the function;  $T$  is the temperature;  $k$  is the heat conducting coefficient;  $c$  is the specific heat capacity;  $\rho$  is the density;  $\lambda$  is the thermal conductivity coefficient;  $x, y, z$  is the variable in the coordinate axis of  $X, Y, Z$ ;  $t$  is the time;  $\theta$  is an adiabatic temperature rise;  $\beta$  is the heat transfer

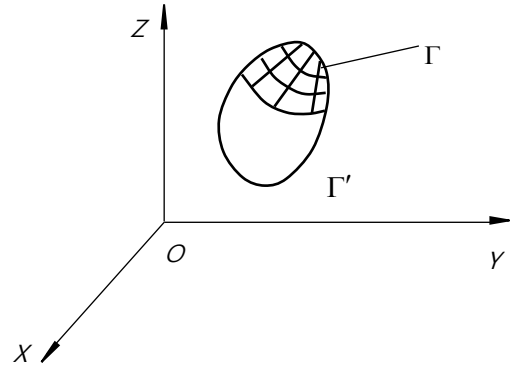


Fig. 2 Space field

coefficient;  $T_a$  is the ambient temperature;  $R$  is the space field;  $\Gamma'$  is the first boundary condition (See Fig. 2.);  $\Gamma$  is the second boundary condition;  $dV$  is the volume of differential;  $d\Gamma$  is the area of differential.

When the function  $I$  takes minimal value, the heat transfer during cement hydration age is written as the following expression

$$\frac{\partial \theta}{\partial t} = \frac{\partial T}{\partial t} - \lambda \nabla^2 T \quad (3)$$

Where,  $\nabla^2$  is the second-order difference operator,  $\theta$  and  $\nabla^2$  which can respectively be expressed as (Zhang 2009, Wang *et al.* 2002)

$$\frac{\partial \theta}{\partial t} = \frac{1}{cp} Q_{\infty} \left( 1 - e^{-\int_{\tau}^{t} m_1 m_2 t^{m_1 - m_3} dt} \right) \quad (4)$$

$$\nabla^2 = \frac{\partial^2}{\partial x^2} + \frac{\partial^2}{\partial y^2} + \frac{\partial^2}{\partial z^2} \quad (5)$$

Where  $Q_{\infty}$  is the maximum hydration heat;  $\tau$  is the initial time of casting concrete;  $m_1, m_2$  and  $m_3$  are the time-dependent coefficients of concrete hydration age, and the value is 0.66, 0.69 and 1.0 respectively.

The Dirichlet boundary condition ( $\Gamma'$ ) can be computed according to the expression

$$T = \bar{T} \quad (6)$$

Where,  $\bar{T}$  is the given temperature in the first boundary condition.

The Neumann boundary condition ( $\Gamma$ ) can be computed according to the expression

$$k \bar{\nabla} T \cdot \bar{n} = \beta (T_a - T) \quad (7)$$

Where,  $\bar{\nabla}$  is gradient vector;  $\bar{n}$  is direction vectors to each coordination axis;  $\beta$  is the coefficient of convection heat transfer (Liu *et al.* 2004).

$$\beta = k_s (5.46v + 6) \quad (8)$$

Where,  $k_s$  is the updated coefficient of convection heat transfer in steel mold,  $k_s = 0.99$ ;  $v$  is the wind speed.

The amount of cement is considered to form the adiabatic temperature rise in the early cement hydration age (Zhu 2013, Wang *et al.* 2002).

$$\frac{\partial \theta}{\partial t} = \frac{Q}{c\rho} = \frac{Wq}{c\rho} \quad (9)$$

Where,  $Q$  is the heat quantity per unit volume concrete;  $W$  is the cement amount and  $q$  is the heat quantity per unit weight cement.

When  $Q$  is supposed to be generated in unit length and time, the energy control equation can be expressed as follow

$$\frac{\partial T}{\partial t} + kT = Q \quad (10)$$

$\frac{\partial T}{\partial t}$  is supposed to present linear change during  $\Delta t$ , and the follow equation is obtained by finite difference method.

$$T_{t+\Delta t} = T_{t-\Delta t} + \left( \frac{\partial T_t}{\partial t} + \frac{\partial T_{t-\Delta t}}{\partial t} \right) \Delta t \quad (11)$$

The Newton-differential equation can be written as

$$k(T_{t+\Delta t} + T_{t-\Delta t}) + \frac{c}{\Delta t}(T_{t+\Delta t} - T_{t-\Delta t}) = (Q_{t+\Delta t} + Q_{t-\Delta t}) \quad (12)$$

To represent the mechanical behavior of concrete at cement hydration age, the following equations needs to be solved

$$\sigma_T(x_i, y_i, z_i) = E_t \alpha (T(x_{i+1}, y_{i+1}, z_{i+1}) - T(x_i, y_i, z_i)) + \sigma_s(x_i, y_i, z_i) \quad (13)$$

Where,  $x_i, y_i, z_i$  is the coordinate;  $\sigma_T(x_i, y_i, z_i)$  is the stress;  $E_t$  is the Modulus elastic at age of  $t$ ;  $\alpha$  is the expansion coefficient;  $T(x_i, y_i, z_i)$  is temperature;  $\sigma_s(x_i, y_i, z_i)$  is structural stress at normal conditions.

### 3. Finite element model

#### 3.1 Details of PC box girder in the Zhaoshi bridge

Fig. 3 shows the massive concrete structure on the pier top of PC continuous box girder with the balance cantilever construction method. Balance cantilever segmental construction for PC box girder bridges has long been recognized as one of the most efficient methods of building bridges without the need of formwork. Construction commences from the permanent piers and proceeds in a balanced manner to the middle span.



Fig. 3 View of box girder on the pier top

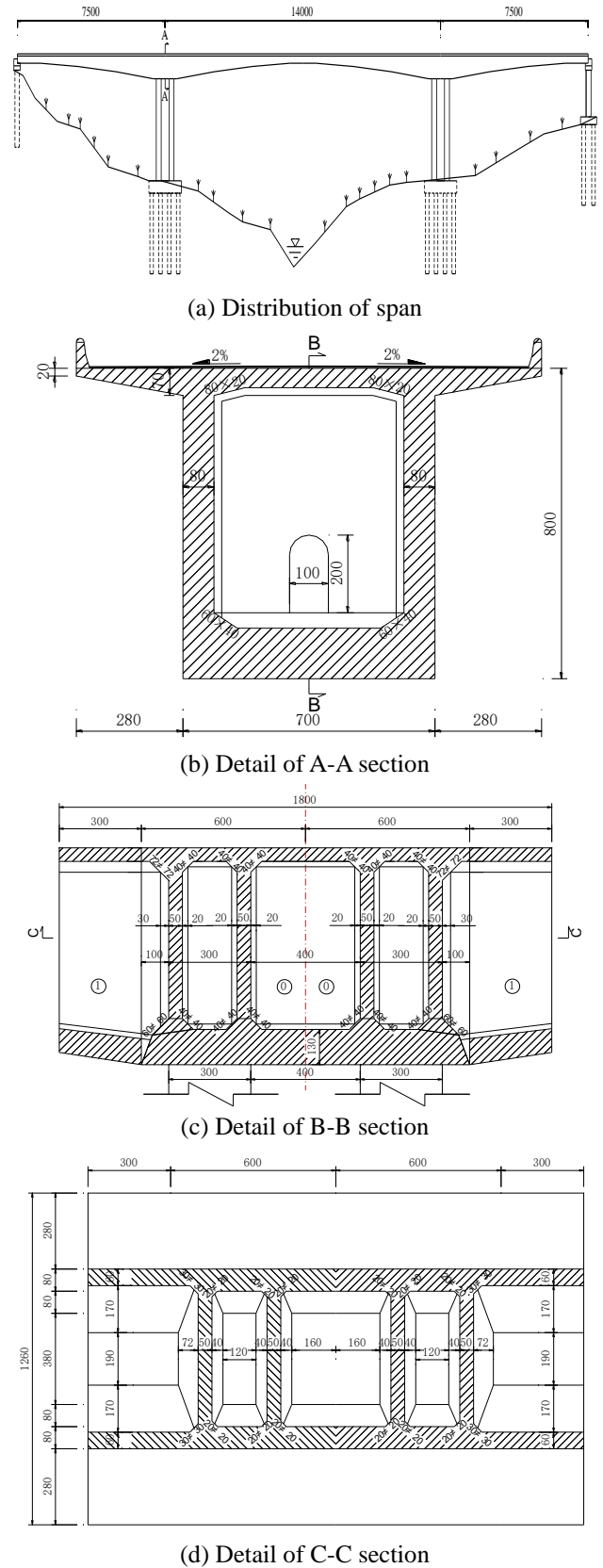


Fig. 4 Details of PC box girder (Unit: cm)

Table 1 Composition of high performance concrete

Constituent	Water	Cement	Sand	Gravel	Mineral powder	Fly ash	Additive
Mixture ratio(kg)	159	476	617	1090	135	85	4.3

Table 2 Elastic modulus and tensile strength of concrete fabricated in box girder at hydration age

Time(hour)	48	96	144	192	240	288	336
Elastic modulus (GPa)	37.0	37.2	37.3	37.4	37.4	37.4	37.5
Tensile strength (MPa)	1.85	2.15	2.38	2.50	2.56	2.64	2.70

Table 3 Material parameters of concrete

Test parameter	Hydration heat per unit weight cement (kJ/kg)	Thermal conductivity (kJ/(m·h·°C))	Specific heat (kJ/(kg·°C))	Initial density (kg/m <sup>3</sup> )	Expansion coefficient
Mean value	350	9.0	0.95	2566.3	1.1×10 <sup>-6</sup>

Fig. 4(a) shows the PC continuous bridge with three-span box girder, whose two side span lengths are 75 m and mid-span length is 140 m. Fig. 4(b) to 4(d) show the details of the cross-sectional dimension of the box girder on the pier top, and the box girder on the pier top has four diaphragms in which one human detection channel is designed. The width of box girder section is 1200 cm, and the height in box girder section on the top of piers is 800 cm. The box girder is assumed to be made of concrete with a design compressive strength (cubic strength) of 50 MPa.

3.2 Concrete material properties

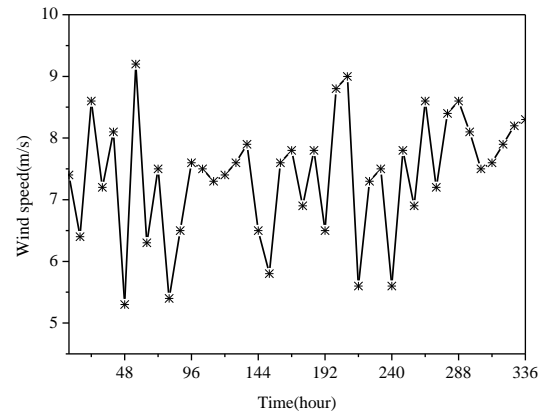
For undertaking sequential thermo-mechanical analysis of PC box girder during curing, thermal and mechanical properties of concrete are to be provided as an input to the finite element model. Table 1 lists the composition of high performance concrete used in the PC box girder. For evaluating elastic modulus and tensile strength of concrete at its early hydration age, concrete prisms were fabricated from concrete batch mix during construction of box girder. Concrete prisms were tested every 24 hours and a summary of representative test data of elastic modulus and tensile strength of concrete are tabulated in Table 2. Thermal properties comprise of hydration heat per unit weight cement, thermal conductivity, specific heat, initial density and expansion coefficient are given in Table 3.

3.3 Wind speed and ambient temperature

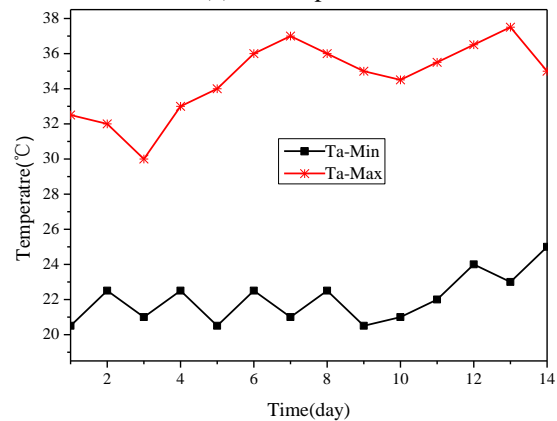
The influence of wind speed and ambient temperature during cement hydration age should be considered due to the fact that convection transfer heat and concrete surface temperature are affected by wind speed and ambient temperature respectively. The wind speed and ambient temperature on the top of piers associated with constructed box girder was monitored by wind speed instrument and temperature sensor throughout the hydration age. The monitored wind and ambient temperature used in thermal analysis of box girder at hydration age are described in Fig. 5.

3.4 Instrument layout

To monitor the distribution of temperature and stress in box girder on the pier top, 20 measuring points were selected in middle section, only a half of these points are

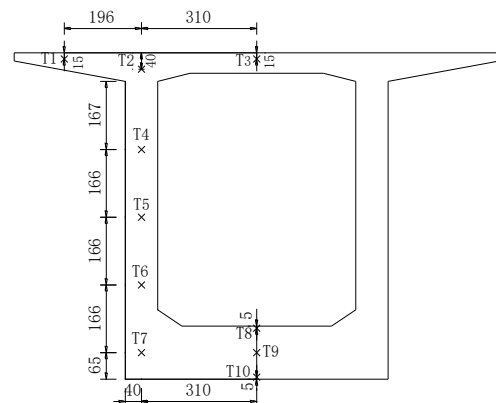


(a) Wind speed



(b) Ambient temperature

Fig. 5 Time-dependent wind speed and ambient temperature monitored in PC box girder at hydration age



(a) Layout of measurement points



(b) Setup of instrument

Fig. 6 Instrument layout

showed in Fig. 6(a), in which T represents testing points of temperature and stress. The measurement lasted for 336 hours from the generation of cement hydration to the decay of cement hydration. Temperature was measured by a new type of electric sensor with high accuracy, high stability, high reliability, moisture proof and good properties of insulation. Fig. 6(b) shows the setup and layout of sensing devices.

### 3.5 Discretization of PC box girder

The PC box girder on the pier top is casted in one time in the order of precedence according to construction process and structural design feature (See Fig. 7(a)). For thermal and structural analysis, the PC box girder is discretized into elements by utilizing different element types available in ANSYS (ANSYS 2012). The box girder has been discretized by means of 85,999 solid elements of revolution (see Fig. 7(b)), each with 4 nodes. The original temperature of concrete at all nodes is set to be the casting temperature, and time-dependent coefficient of convection heat transfer and curing temperature (ambient temperature) are provided as input into ANSYS every 8 hours.

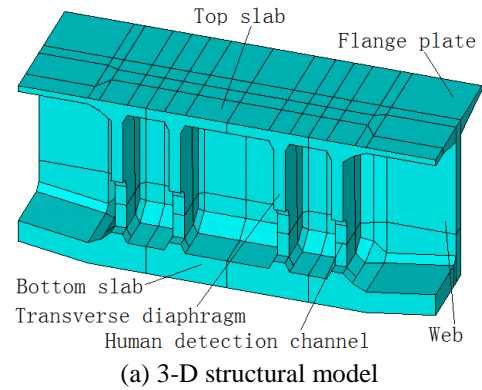
The heat transfer analysis in the concrete box girder is carried out by using SOLID70 element. SOLID70 is a 3-D element with three-dimensional thermal conduction capability and has eight nodes, with a single degree of freedom at each node, namely temperature. This element is well suited to three-dimensional transient thermal analysis problem.

For structural analysis, the bottom slab, web, top slab, flange plate and transverse diaphragms were modeled with SOLID65 elements. SOLID65 has eight nodes with three degrees of freedom per node, namely three translations in the nodal x, y, z directions. This element can be applicable for three-dimensional modeling of solids and is capable of accounting for plasticity, stress stiffening, creep, large deflection, and large strain effects.

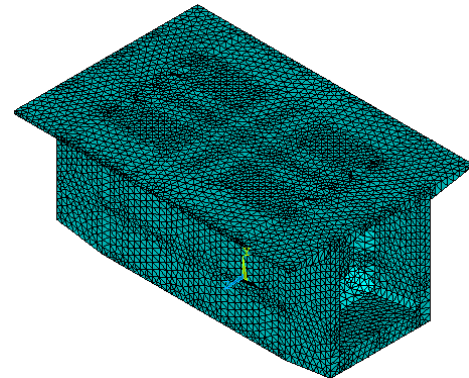
Thermo-mechanical analysis can be regarded as an interaction between temperature and stress, which the same model and meshing were applied to the thermal and structural analysis. Temperatures generated from thermal analysis were applied as a thermal-body-load on the structural elements to simulate conditions of concrete box girder during its early hydration age. The temperature-dependent mechanical properties of concrete, namely, tensile strength and elastic modulus, are assumed to follow as that of Table 2, and these properties as input data are provided into ANSYS program. In addition, time-dependent wind speed and ambient temperature are assumed to follow as that of Fig. 5.

### 3.6 Thermal analysis

Fig. 8 shows the comparison between the predicted and measured temperature of cement hydration heat in concrete box girder at representative measuring points T1 and T7, which are located in the structure edge and the center of massive concrete respectively. Temperature evolutions in other measuring points are assumed to have similar trend to that of these two points. It can be seen from the curves that

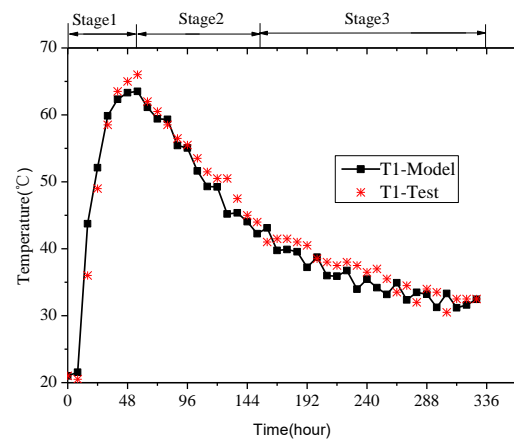


(a) 3-D structural model

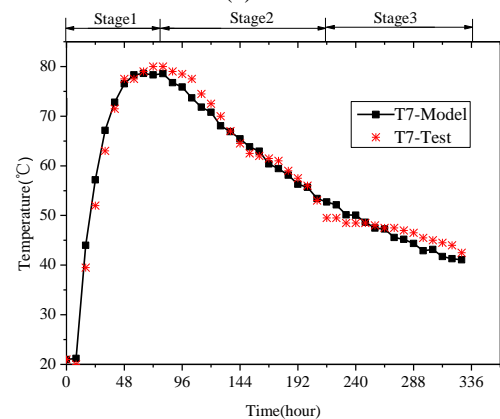


(b) Three-dimensional discretization

Fig. 7 FEM of PC box girder for analysis



(a) T1



(b) T7

Fig. 8 Comparison between the predicted and measured temperatures

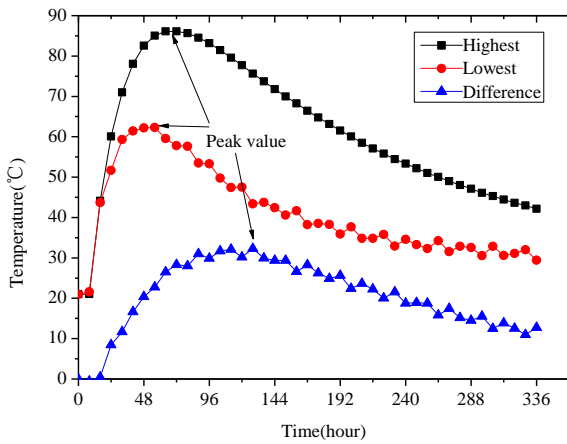


Fig. 9 Evolution of maximum and minimum temperature and temperature difference

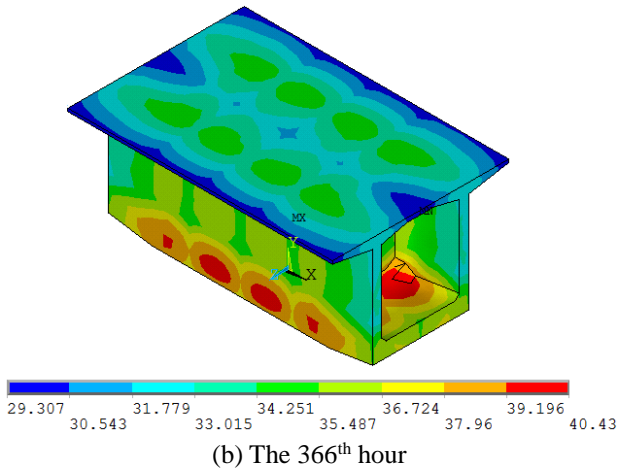
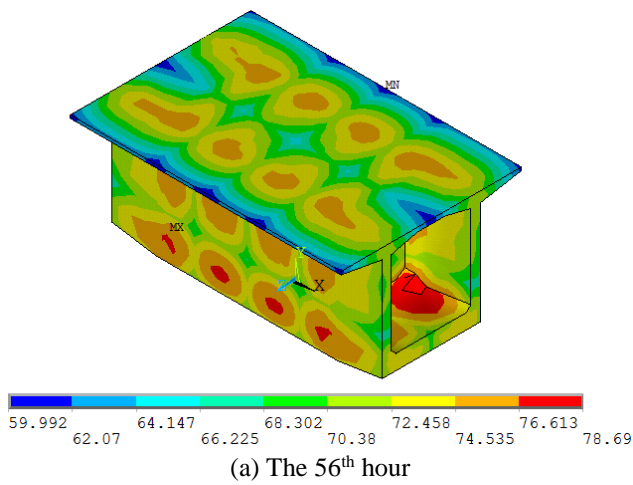
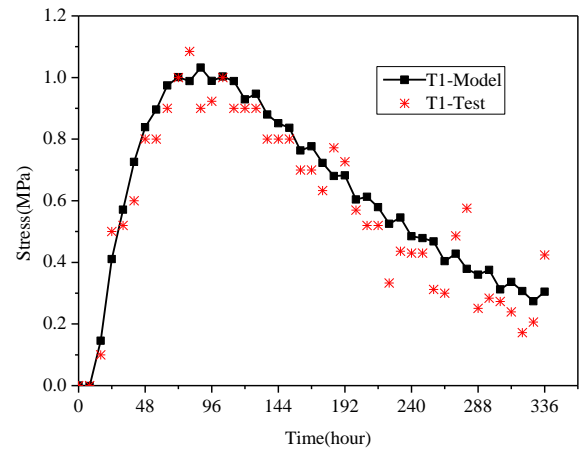
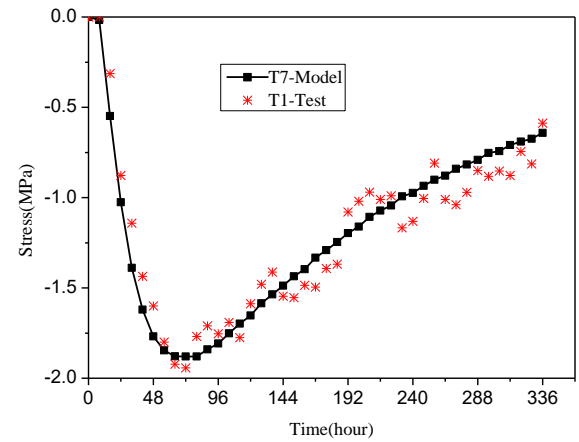


Fig. 10 Three-dimensional distribution of temperature in the box girder from cement hydration heat

the predicted temperatures agree well with the measured results, indicating that the three-dimensional finite element program presented in this study can be applied to solve actual problems. The slight differences can be mainly attributed to variation of the heat transfer parameters such as coefficients of convection heat transfer and non-homogeneous characteristics of concrete material used in the analysis as compared to actual values encountered in the



(a) T1



(b) T7

Fig. 11 Comparison between the predicted and measured stresses along x-axis in measuring points

experiments.

There are three stages to elucidate the temperature progression of cement hydration heat of concrete box girder in Fig. 8(a), namely Stage 1, Stage 2 and Stage 3. In Stage 1 (about 56 hour), temperature increases with a rapid pace due to the fact that reaction between cement particles and water generates large amount of hydration heat in the initial phase. In Stage 2 (between 56 hour and 156 hour), temperature starts to decrease with a low pace mainly resulting from termination of hydration reaction in cement. In Stage 3 (after 156 hour), temperature decreases much slowly due to poor heat transfer performance and lower thermal gradient within girder body. The temperature progression of cement hydration heat in Fig. 8(b) is similar to that in Fig. 8(a), except that time corresponding to each stage is different, namely, from 0 to 80 hour in Stage 1, 80 hour to 216 hour in Stage 2, and 216 hour to 336 hour in Stage 3.

Fig. 9 shows an evolution of the highest and lowest temperature and maximum temperature difference in the PC box girder. It can be seen that the trend of temperature progression in these curves is similar to that in Fig. 8. The degradation stage in the lowest temperature presents a little fluctuation due to influence of ambient temperature. The peak value of the highest temperature is 86°C, which occurs in 72 hour. The peak value of the lowest temperature is

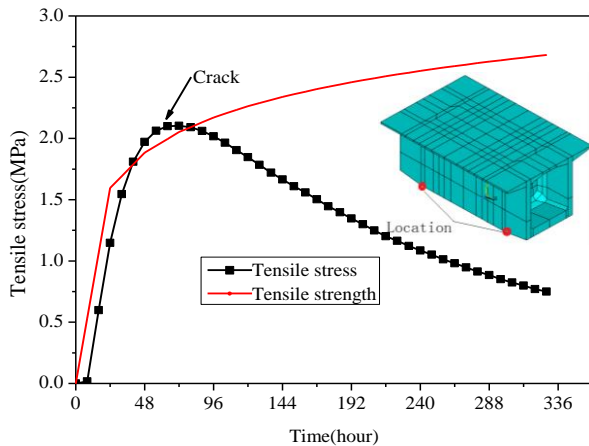


Fig. 12 Progression and location of the crack in PC box girder at hydration age

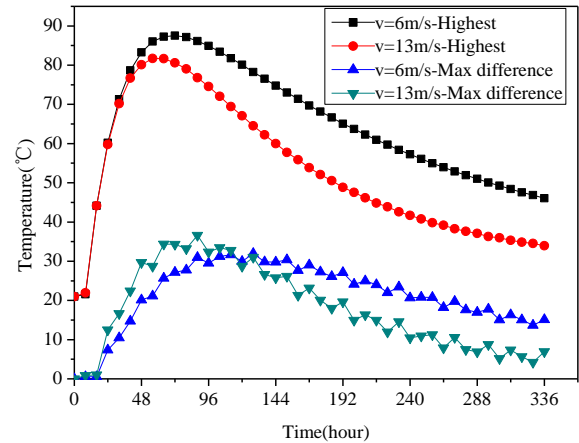
62°C, and its occurrence time is 56 hour, earlier than that of the highest temperature. The maximum temperature difference is about 32°C, and its occurrence time is 120 hour.

Fig. 10 shows a three-dimensional temperature distribution of concrete box girder on the pier top at hydration age through numerical model. It can be seen that temperatures in two portions are higher than temperatures in other parts, namely the location of web, bottom slab and transverse diaphragm and the location of web, top slab and transverse diaphragm. The temperature has a slight degradation from the intercourse location to the edge of the structure. At the 56<sup>th</sup> hour, the highest temperature, 79°C, is located in the intercourse portion, while the lowest temperature, nearly 60°C, is located in the edge of flange plate, due to the fact that the flange plate has thin concrete in the edge and large area of convection heat transfer. At the 336<sup>th</sup> hour, the highest temperature is 40°C and the lowest temperature is 29°C. The 3-D distribution of temperatures in the box girder from cement hydration heat depends on hydration age.

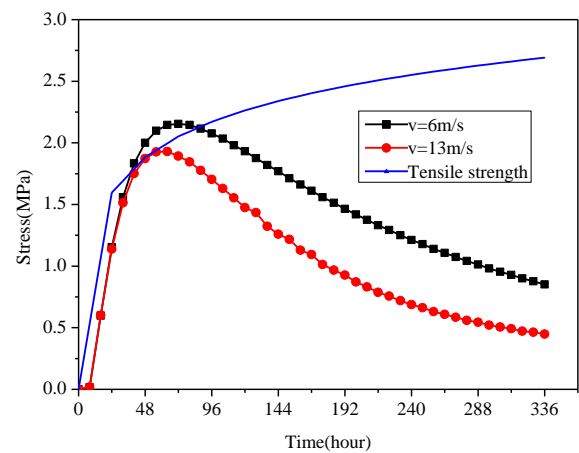
### 3.7 Thermo-mechanical analysis

Fig. 11 shows the comparison between the predicted and measured stress along x-axis of cement hydration in concrete box girder at representative measuring points T1 and T7. The predicted value shows a good qualitative and quantitative agreement with the experimental values at points T1 and T7. A slight difference can be mainly attributed to influence of dry shrinkage.

Fig. 12 shows a progression and location of the crack in PC box girder at hydration age. It can be seen that the trend of the maximum principle tensile stress is similar to that of the highest temperature, and occurrence time (72 hour) of peak value in the principle tensile stress is identical to that of the highest temperature. When the principle stress is larger than the tensile strength of concrete, cracking happens and the history time of crack is between 40 hour and 88 hour. The crack is located in the region of piers and bottom slab and the outside transverse diaphragm, this is mainly due to excessive thermal strain and deformation



(a) Highest temperature and maximum temperature difference



(b) Maximum tensile stress

Fig. 13 Progression of temperature and stress in PC box girder at hydration age with different wind speed

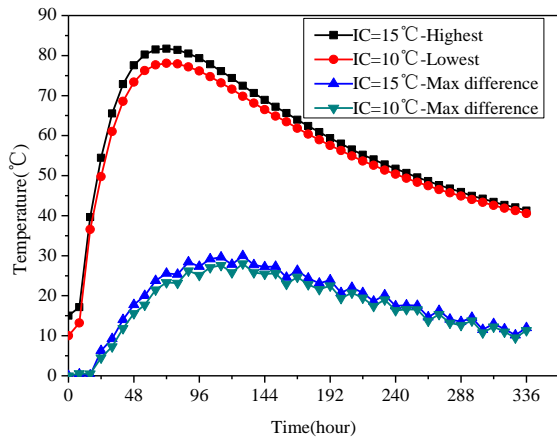
limit of extra constraint in the structure.

## 4. Parametric analysis

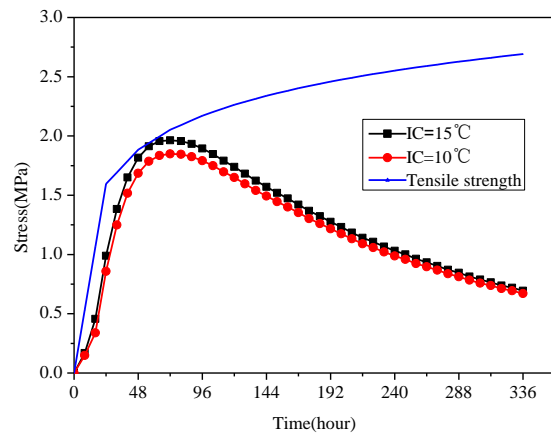
The validated finite element model is applied to quantify the effect of different parameters on progression of temperature rise and stresses in PC box girder during curing. Wind speed, pre-cooling temperature and curing temperature are selected for parametric analysis.

### 4.1 Wind speed

To understand the influence of the wind speed on the maximum principle tensile stress of PC box girder on the pier top, the wind speed is assumed to be 6 m/s and 13 m/s respectively. Fig. 13(a) shows a progression of the highest temperature and maximum temperature difference with different wind speed. It can be seen that the highest temperature and maximum temperature difference can be reduced by elevation of wind speed. Fig. 13(b) indicates that bigger wind speed can reduce the maximum principle tensile stress in PC box girder. This may be attributed to the reason that bigger wind speed can accelerate the spread of hydration heat.



(a) Highest temperature and maximum temperature difference



(b) Maximum tensile stress

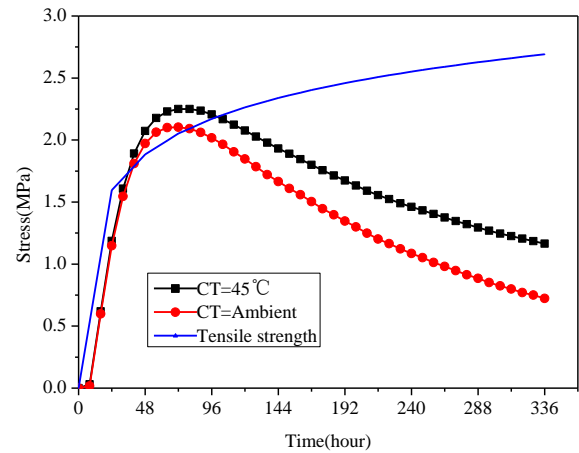
Fig. 14 Progression of temperature and stress in PC box girder under different initial casting temperature

#### 4.2 Pre-cooling temperature

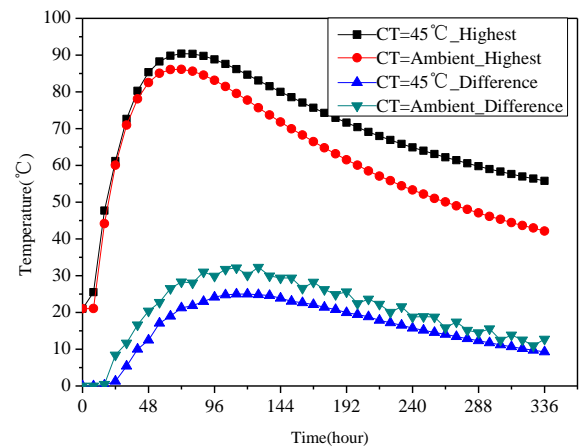
Pre-cooling technique can reduce the initial casting (IC) temperature. The IC temperature is assumed to be 15°C and 10°C respectively. Fig. 14(a) shows a progression of the highest temperature and maximum temperature difference in PC box girder at hydration age under different casting temperature. It can be seen that the highest temperature and maximum temperature difference can be reduced by decrease of initial casting temperature. From Fig. 14(b), the effect of IC temperature on the maximum principle tensile stress in PC box girder can be determined. When the IC temperature decreases from 15°C to 10°C, the maximum tensile stress is totally reduced during the hydration process of the PC box girder, and the most distinct decrease of the maximum tensile stress occurs between 40 hour and 88 hour, consistent with the history time of crack. Therefore, decreasing the initial casting temperature can effectively reduce the maximum tensile stress in the critical period and thus prevent the occurrence of cracking.

#### 4.3 Curing temperature

Effect of the curing temperature (CT) of structural surface on the maximum principle tensile stress of PC box



(a) Highest temperature and maximum temperature difference



(b) Maximum tensile stress

Fig. 15 Progression of temperature and tensile stress in PC box girder under different curing temperatures

girder on the pier top is discussed. The CT temperature is assumed to be 45°C and ambient temperature respectively. Fig. 15(a) shows that the maximum temperature difference can be reduced by increase of CT, but the highest temperature increases. Fig. 15(b) shows a progression of the maximum principle tensile stress under curing temperature 45°C and ambient temperature. The maximum principle stress increases when the curing temperature enhances from ambient temperature to 45°C, so increasing the curing temperature is detrimental to prevent cracking.

## 5. Conclusions

A numerical simulation procedure for evaluating the behavior of PC box girder during the early hydration age has been proposed in this study. A time-dependent wind speed and ambient temperature is incorporated into finite element to trace the crack history and location in PC box girder. A parametric analysis was performed to show the effect of different parameters on thermal and mechanical response of PC box girder on pier top, namely the wind speed, the initial casting temperature and the curing temperature.

- From the comparison between the predicted results and experimental data, it can be seen that the developed finite element program well predicts the temperature evolution of PC box girder on pier top at cement hydration age.
- The wind speed has an influence on the path in the degradation stage of temperature and stress, and it can obviously change the peak value of temperature and stress.
- The initial casting temperature can significantly affect the maximum tensile stress in the PC box girder. So reducing the initial casting temperature by pre-cooling technique is an effective measure to control cracking in PC box girders.
- Increasing the curing temperature can reduce the maximum temperature difference, whereas enhance the highest temperature. Generally, increasing the curing temperature is detrimental to prevent cracking.

## Acknowledgments

The research described in this paper was financially supported by the National Natural Science Foundation of China under Grant Number 51308056, China Scholarship Fund under Grant Number 201406565013, research Fund for the Central Universities of China under Grant Number 310821172003.

## References

- ANSYS (2012), *ANSYS Metaphysics (Version 14.0)*, ANSYS Inc.
- Chummuneerat, S., Jitsangiam, P. and Nikraz, H. (2014), "Performances of hydrated cement treated crushed rock base for western Australian roads", *J. Traff. Transp. Eng.*, **1**(6), 432-438.
- EI-Tayeb, E.H., EI-Metwally, S.E., Askar, H.S. and Yousef, A.M. (2017), "Thermal analysis of reinforced concrete beams and frames", *Hbrc J.*, **13**(1), 8-24.
- Estrada, C.F., Godoy, L.A. and Prato, T. (2006), "Thermo-mechanical behavior of a thin concrete shell during its early age", *Thin Wall Struct.*, **44**(5), 483-495.
- Fairbairn, E.M.R., Silvosio, M.M., Filho, R.D.T., Alves, J.L.D. and Ebecken, N.F.F. (2004), "Optimization of mass concrete construction using genetic algorithms", *Comput. Struct.*, **82**(2-3), 281-299.
- Germaniuk, K., Gajda, T., Sakowski, A., Weirzbicki, T. and Kamiński, P. (2016), "Bridge structures cracks-what made that phenomena so common?", *Transp. Res. Proc.*, **14**, 4030-4039.
- Gilbert, R.I. (2017), "Cracking caused by early-age deformation of concrete-prediction and control", *Proc. Eng.*, 13-22.
- Jin, K.K., Kim, K.H. and Yang, J.K. (2001), "Thermal analysis of hydration heat in concrete structures with pipe-cooling system", *Comput. Struct.*, **79**(2), 163-171.
- Kodur, V.K.R., Bhatt, P.P., Soroushian, P. and Arablouei, A. (2016), "Temperature and stress development in ultra-high-performance concrete during curing", *Constr. Build. Mater.*, **122**, 63-71.
- Krkoška, L. and Moravčík, M. (2015), "The analysis of thermal effect on concrete box girder bridge", *Proc. Eng.*, **111**, 470-477.
- Kuriakose, B., Rao, B.N. and Dodagoudar, G.R. (2016), "Early-age temperature distribution in a massive concrete foundation", *Proc. Tech.*, **25**, 107-114.
- Liu, W.Y., Huang, D.Y. and Hua, Y.J. (2004), "Probe into test method of heat convection coefficient of concrete", *Sich. Build. Sci.*, **12**(4), 87-89.
- Pepe, M., Koenders, E.A.B., Faella, C. and Martinelli, E. (2014), "Structural concrete made with recycled aggregates: Hydration process and compressive strength models", *Mech. Res. Commun.*, **58**, 139-145.
- Schackow, A., Effting, C., Gomes, I.R., Patrui, I.Z., Vicenzi, F. and Kramel, C. (2016), "Temperature variation in concrete samples due to cement hydration", *Appl. Therm. Eng.*, **103**, 1362-1369.
- Schutter, G.D. and Vuylsteke, M. (2004), "Minimisation of early age thermal cracking in a J-shaped non-reinforced massive concrete quay wall", *Eng. Struct.*, **26**(6), 801-808.
- Wang, Z.B., Wang, X.D. and Xu, D.Y. (2002), "Imitated analysis of thermal stresses in concrete structure", *J. Nanj. Univ. Technol.*, **24**(5), 20-24.
- Wang, D., Shi, C., Wu, Z., Xiao, J., Huang, Z. and Fang, Z. (2015), "A review on ultra-high-performance concrete: Part ii. Hydration, microstructure and properties", *Constr. Build. Mater.*, **96**, 368-377.
- Yi, T.H., Li, H.N. and Sun, H.M. (2013a), "Multi-stage structural damage diagnosis method based on "energy-damage" theory", *Smart Struct. Syst.*, **12**(3-4), 345-361.
- Yi, T.H., Li, H.N. and Gu, M. (2013b), "Experimental assessment of high-rate GPS receivers for deformation monitoring of bridge measurement", *J. Int. Meas. Confederat.*, **46**(1), 420-432.
- Yi, T.H., Li, H.N. and Zhang, X.D. (2012), "A modified monkey algorithm for optimal sensor placement in structural health monitoring", *Smart Mater. Struct.*, **21**(10), 1-9.
- Yun, L. and Kim, J.K. (2009), "Numerical analysis of the early age behavior of concrete structures with a hydration based microplane model", *Comput. Struct.*, **87**(17-18), 1085-1101.
- Zhang, G. (2009), "Analysis of thermo-mechanics tempo-spatial effect for concrete bridges on heat conduction model of fluid-solid coupled and safety evaluation", Ph.D. Dissertation, Changan University, Xi'an, China.
- Zhu, B.F. (2013), *Thermal Stresses and Temperature Control of Mass Concrete*, Butterworth-Heinemann, London, U.K.

HK